Adsorption of End-Functionalized Polymers on Colloidal Spheres

B. L. Carvalho,† P. Tong,*,‡ J. S. Huang,§ T. A. Witten,‖ and L. J. Fetters§

*Department of Materials Science and Engineering, Massachusetts Institute of Technology,
Cambridge, Massachusetts 02139, Department of Physics, Oklahoma State University,
Stillwater, Oklahoma 74078, Exxon Research and Engineering Company,
Annandale, New Jersey 08801, and The James Franck Institute, University of Chicago,
5640 S. Ellis Avenue, Chicago, Illinois 60637*

ABSTRACT: We report a light scattering study of the adsorption of end-functionalized polymers on colloidal spheres. A light scattering method is developed to measure the amount of polymer molecules adsorbed on the colloidal surfaces. The experiment reveals that only a fraction of the end-functionalized polymers is adsorbed on the colloidal surface. The results for the end-functionalized polymers are compared with those for the unfunctionalized polymer. It is found that the interaction between the colloid and the unfunctionalized polymer is repulsive, which introduces a depletion attraction between the colloidal particles. The functional end groups are found to interact attractively with the polar cores of the colloidal particles. The adsorption energy between the functional group and the colloidal surface is estimated to be $\sim 4k_BT$. The experiment shows that the presence of the adsorbed polymer on the colloidal surfaces greatly reduces the depletion attraction between the colloidal particles and, therefore, enhances the stability of the colloid–polymer mixture.

1. Introduction

The stability of colloidal suspensions in polymer solutions has been a subject of many experimental and theoretical investigations. The study of such complex systems has a myriad of industrial applications. Lubricating oils and paint are examples of colloid–polymer mixtures where phase stability is desired. Water contaminated with colloidal impurities represents a situation where it is hoped that the addition of a small amount of polymer can induce colloidal particles to flocculate, thereby allowing for the easy removal of the colloidal impurities. The complexity of these systems arises because of the formation of an adsorption (or depletion) layer of polymers at the surface of the colloidal particles. This adsorption (or depletion) layer changes the colloid–colloid interaction potential $U(r)$, which is the work required to bring two colloidal particles from infinity to a separation r under a given solvent condition. The potential $U(r)$ determines the osmotic pressure of a stable colloidal dispersion. It also governs the stabilities of such systems.[1,2]

It is important to distinguish between polymers which are adsorbed on the colloidal surface and those that are free in solutions because the two situations usually lead to quantitatively different effects. In the latter case the exclusion of free polymer molecules from the interparticle space results in an attractive force between the colloidal particles.[3] If the attraction is large enough, phase separation or flocculation of the colloidal particles occurs. This depletion effect was first recognized by Asakura and Oosawa,[4] and in recent years, many theoretical and experimental studies of the depletion effect have been carried out in various aqueous and organic colloidal solutions. Most experimental studies, however, are restricted to examining the phase behavior of the colloid–polymer mixtures. Recently, we developed a light scattering approach to probe changes of the interaction potential $U(r)$ between the colloidal particles in a free polymer solution.[5] In our experiment, the second virial coefficient of the colloidal particles as a function of the free-polymer concentration was obtained from measure-

ments of the concentration dependence of the light intensity scattered from the mixture. The experiment demonstrates that the light scattering scheme is indeed capable of measuring the depletion effect in the colloid–polymer mixture.

In the case of adsorption, the adsorbed polymer, in a good solvent, resists the approach of other surfaces through a loss of conformational entropy. Surfaces, then, are maintained at separations large enough to damp any attractions due to the depletion effect or London–van der Waals force, and the colloidal suspension is stabilized. The adsorbed polymer layer affects not only the thermodynamics but also the hydrodynamics of the colloidal solution.[1,2] Dynamic light scattering has been used to estimate the apparent hydrodynamic thickness of an adsorbed polymer layer.[6] The hydrodynamic thickness is the difference between the Stokes' radius of the bare colloidal particle in the solvent alone and the value for the particle in the polymer solution. While it is straightforward to perform a dynamic light scattering measurement on a mixture of colloid and polymer, any determination of the hydrodynamic thickness requires all the polymer molecules to stick on the colloidal surfaces.

In this paper we report a static light scattering study of the adsorption of end-functionalized polymers on colloidal spheres. A scattering method is developed to measure the fraction of the polymer molecules with their end-group anchored to the colloidal surfaces. The colloidal particle chosen for the study consists of a calcium carbonate ($CaCO_3$) core with an adsorbed monolayer of a randomly branched calcium alkylbenzene sulfonate (CaSA) surfactant. The 10-nm-diameter colloidal particles are dispersed in decane. Monodispersed hydrogenated polyisoprene and its single-end-functionalized derivatives with molecular weights of 25 000 are used to modify the interaction between the polymer and the colloid. Such a nonaqueous colloid–polymer mixture is ideal for the investigation attempted here since the colloidal system is approximately a hard-sphere system, and both the colloid and the polymer have been well-characterized previously using various experimental techniques (see section 3).

It is found that only a fraction of the end-functionalized polymers adsorbs on the colloidal surface. The adsorption energy between the functional group and the colloidal surface is estimated to be $\sim 4k_BT$. The results for the end-functionalized polymers are compared with those for

* Author to whom all correspondence should be addressed.
† Massachusetts Institute of Technology.
‡ Oklahoma State University.
§ Exxon Research and Engineering Co.
‖ University of Chicago.

the unfunctionalized polymer. Because the unfunctionalized polymer does not adsorb, at all, to the colloidal spheres, we view the adsorption of the end-functionalized polymer as occurring through the functional end group. The experiment shows that the adsorption of the polymer colloidal surfaces greatly reduces the depletion attraction between the colloidal particles. However, there is still some residual attraction between the colloidal particles due to the unadsorbed polymer molecules in the solution. The experiment is of interest to observe the microscopic interaction between the colloid and polymer and to see how it responds to the incorporation of a functional group on the polymers. With this knowledge, one can estimate the phase stability properties of colloid–polymer mixtures in a straightforward way. (The reverse process of inferring the elementary interactions from the phase behavior is much more problematic and unsure.)

The paper is organized as follows. Section 2 presents the calculation for the adsorption energy ϵ and describes the light scattering method used in the experiment. Experimental details appear in section 3, and the results are discussed in section 4. Finally the work is summarized in section 5.

2. Theory

2.1. Estimation of the Adsorption Energy ϵ. The adsorption of the end-functionalized polymer chains on the colloidal surfaces leads to the formation of colloid–polymer complexes of various sizes. The colloid–polymer complex can be viewed as a polymer micelle with colloidal particles surrounded by polymer molecules. When the adsorption energy ϵ between the end-functional group and the colloidal surface is not much larger than k_BT, only a fraction of the polymer molecules can anchor to the colloidal surface. In this case the colloid–polymer mixture is a three-solute system consisting of polymer–colloid micelles, free polymer molecules, and bare colloidal particles. For dilute solutions with negligible intermicellar interactions, the size distribution of the polymer–colloid micelles can be written as[7]

$$x_n = x_c [x_p e^{-\Delta\mu_n^0/k_BT}]^n \qquad (1)$$

where x_n is the mole (number) fraction of the polymer–colloid micelles with an aggregation number n, and x_p (x_c) is the number fraction of the free polymer molecules (the bare colloidal particles) in the solution. In the above, k_B is Boltzmann's constant, T is the absolute temperature, and $\Delta\mu_n^0$ is the standard free energy change per polymer molecule when n polymer molecules associate to form a polymer–colloid micelle. Equation 1 states that the probability of finding an n-mer polymer–colloid micelle is simply a product of two factors. The first factor $x_c x_p^n$ is the probability of finding n polymer chains surrounding a single colloidal particle. The second factor $e^{-n\Delta\mu_n^0/k_BT}$ is a Boltzmann factor that accounts for the free energy changes when the n polymer chains adsorb onto the colloidal particle. The overall number fractions of polymer X_p and colloid X_c are given by the mass conservation relations

$$X_p = x_p + \sum_{n=1}^{\infty} n x_n \qquad (2)$$

and

$$X_c = x_c + \sum_{n=1}^{\infty} x_n \qquad (3)$$

The above equations have been used to study the aggregation of mixed micelles[8] and microemulsions.[7] Given

the free energy difference $\Delta\mu_n^0$, eqs 1–3 completely determine the distribution of the polymer–colloid micelles in mixtures of colloids and end-functionalized polymers. In the experiment to be discussed below, both the free polymer concentration and the surface coverage of the adsorbed polymer are below the overlap polymer concentration, so that one can ignore the excluded-volume interaction between the polymer chains. In this dilute limit, the free energy difference $\Delta\mu_n^0$ can be written as

$$\Delta\mu_n^0 = -\epsilon + T\Delta S \qquad (4)$$

In the above, ϵ is the adsorption energy between the end-functional group and the colloidal surface, and ΔS is the change of the conformational entropy for a free polymer chain to attach to the colloidal surface.

The total number of configurations for a free polymer chain in a good solvent scales[9] as $\bar{z}^N N^{\nu-1}$, where N is the degree of polymerization, $\bar{z}$ is an effective coordination number, and $\nu = 7/6$ for three-dimensional lattices. A computer simulation by Eisenriegler et al.[10] has shown that for a polymer chain with its one end fixed at a flat wall, otherwise in a good solvent, the number of configurations has the same scaling form as for a free polymer chain but with $\nu = 0.695$. Therefore, the probability of finding a polymer chain with its one end fixed at a flat wall is $\Psi(N) = \Psi_0 N^{-\nu'}$, where the exponent $\nu' = 7/6 - 0.695 = 0.472$. The proportionality constant Ψ_0 should be of order unity because $\Psi(N = 1) = 1$. The change of conformational entropy then has the form

$$\Delta S = -k_B \ln \Psi(N) = 0.472 k_B \ln N \qquad (5)$$

Incorporating eqs 1, 4, and 5 into eqs 2 and 3, we have

$$X_c = \frac{x_c}{1 - x_p e^{-\Delta\mu_n^0/k_BT}} \qquad (6)$$

and

$$X_p = x_p \left[1 + \frac{X_c e^{-\Delta\mu_n^0/k_BT}}{1 - x_p e^{-\Delta\mu_n^0/k_BT}} \right] \qquad (7)$$

with

$$\Delta\mu_n^0 = -\epsilon + 0.472 k_B T \ln N \qquad (8)$$

In the above, we have made use of the identities $\sum_{n=1}^{\infty} y^n = y/(1-y)$ and $\sum_{n=1}^{\infty} n y^n = y/(1-y)^2$. For dilute polymer solutions, eq 7 can be rewritten as

$$\frac{\alpha}{1-\alpha} \equiv \frac{X_p - x_p}{x_p} \simeq X_c e^{-\Delta\mu_n^0/k_BT} \qquad (9)$$

where α is the number fraction of the adsorbed polymer to the total number of the polymer molecules, and $1 - \alpha$ is the number fraction of the free polymer. Equation 9 states that, in the weak adsorption limit, the partition coefficient α, which is the probability for a single polymer chain to anchor to the colloidal surface, is proportional to the Boltzmann factor $e^{-\Delta\mu_n^0/k_BT}$. For the polymer adsorption, the proportionality constant X_c in eq 9 should be the ratio of the available "adsorption volume" (the total area of the colloidal surfaces times the adsorption layer thickness δ) to the total volume of the sample. This ratio describes the loss of translational entropy for the adsorbed polymer chains. Therefore, we have $X_c = 3\phi_1\delta/R_{11}$, where ϕ_1 is the volume fraction of the colloidal particles, and R_{11} is their radius.

Using eq 9, one can solve for the adsorption energy ϵ, that must be supplied to the polymer in order to adsorb

on the colloidal surfaces,

$$\epsilon = k_B T \left\{ 0.472 \ln N - \ln X_c - \ln\left(\frac{1-\alpha}{\alpha}\right) \right\} \qquad (10)$$

In the case where the unadsorbed polymer molecules in the solution form polymer micelles without a colloidal core, the above derivation is still valid since the polymer micelle is just another species to replace the free polymer chains. The critical micellar concentration for our polymer is so low[11] that we can ignore the free polymer chains in this case. Equation 10 then becomes

$$\epsilon - f_0 = k_B T \left\{ 0.472 \ln N - \ln X_c - \ln\left(\frac{1-\alpha}{\alpha}\right) \right\} \qquad (11)$$

In the above, $f_0(p,N)$ is the free energy of a single polymer chain in a polymer aggregate, with p being the aggregation number and N being the degree of polymerization of the polymer chains. Bug et al.[12,13] have calculated $f_0(p,N)$ for spherical polymer aggregates. Here we treat f_0 as a constant because there are some unknown numerical parameters in estimating f_0.[12]

2.2. Scattering from a Mixture of Colloid and Polymer.
It has been shown[5,14] that the scattering intensity from a mixture of colloid and nonadsorbing polymer can be written as

$$I(\mathbf{Q}) \sim \rho_1 f_1^2(\mathbf{Q}) \, S_{11}(\mathbf{Q}) + 2(\rho_1\rho_2)^{1/2} f_1(\mathbf{Q}) \, f_2(\mathbf{Q}) \, S_{12}(\mathbf{Q}) +$$
$$\rho_2 f_2^2(\mathbf{Q}) \, S_{22}(\mathbf{Q}) \qquad (12)$$

where ρ and $f(\mathbf{Q})$ are the number density and the scattering form factor, respectively. Here the colloidal particle is denoted as component 1, while the polymer molecule is denoted as component 2. The scattering vector $\mathbf{Q}$ has an amplitude $Q = (4\pi/\lambda) \sin(\theta/2)$, where λ is the wavelength of the light in the liquid solvent, and θ is the scattering angle. The partial structure factor $S_{ij}(\mathbf{Q})$ measures the particle interaction between components i and j. For the colloid–polymer mixtures studied here, the scattering from a colloidal particle is much stronger than that from a polymer molecule, so that the polymer solution can be treated as a solvent. With this assumption eq 12 can be rewritten as[5]

$$BM_1\rho'_1/R(0) = Y(\rho'_2) + \frac{2\rho'_1}{M_1} P(\rho'_2) \qquad (13)$$

where the intercept

$$Y(\rho'_2) = 1 - \frac{\rho'_2}{M_2} \frac{2f_2}{f_1} C_{12} - \left(\frac{\rho'_2}{M_2}\right)^2 \left\{ \frac{2f_2}{f_1} (C_{12}C_{22} + E_2) - \left(\frac{f_2}{f_1}\right)^2 (3C_{12}^2 - B_1) \right\} + \mathcal{O}(\rho_2^3) \qquad (14)$$

and the slope

$$P(\rho'_2) = -\frac{C_{11}}{2} - \frac{\rho'_2}{2M_2}\left\{ (C_{12}^2 + A_2) - \frac{2f_2}{f_1}(C_{12}C_{11} - E_1) \right\} + \mathcal{O}(\rho_2^2, \rho_1) \qquad (15)$$

In the above, M is the molecular weight, $\rho' \equiv \rho M$ is the mass density (g/cm³), and $B = B'(f_1/M_1)^2$, with B' being a proportionality constant. The excess intensity $R(0)$ is defined as $I(0) - I_0$, where $I(0)$ is the scattered intensity from the mixture at concentrations ρ'_1 and ρ'_2, measured at the scattering angle $\theta = 0$, and I_0 is the scattering intensity of the polymer solution alone ($\rho'_1 = 0$). The coefficients in eqs 14 and 15 are the density-expansion coefficients for $S_{ij}(\mathbf{Q})$, with $-C_{ij}/2$ being the second virial

coefficients and A_2, B_1, E_1, and E_2 being the higher-order expansion coefficients. These coefficients have been calculated in ref 5.

If the polymer is invisible ($f_2 = 0$), $P(\rho'_2)$ in eq 15 becomes an effective second virial coefficient $b_{11}(\rho'_2)$ of the colloidal particles at a given polymer concentration ρ'_2. This virial coefficient has the usual interpretation in terms of osmotic pressure derivatives. Equation 15 states that the interaction between a colloidal particle and a polymer molecule reduces the value of $b_{11}(\rho'_2)$, and therefore the effective interaction between the colloidal particles may become attractive if enough polymer is added. When the polymer is visible ($f_2 \neq 0$), the interference between the two species changes both the intercept Y and the slope P. From the measured $Y(\rho'_2)$ the colloid–polymer interaction parameter C_{12} can be obtained using eq 14. Therefore, we can find quantitatively how the two species attract or repel. Experimentally, a straight line can be obtained at the low ρ'_1 end when the measured $\rho'_1/R(0)$ is plotted against ρ'_1. From the intercept and the slope of the straight line one obtains C_{12} and $b_{11}(\rho'_2)$.

The two independent variables used in eq 13, which determine the total scattering intensity of the colloid–polymer mixture, are the concentrations of colloid ρ'_1 and polymer ρ'_2. Sometimes one may find it more convenient to work with the polymer-to-colloid molar ratio $\omega = \rho_2/\rho_1$, instead of ρ_2. When ρ_2 is replaced by $\omega\rho_1$, eqs 14 and 15 become

$$Y(\omega) = \frac{1}{1 + (f_2/f_1)^2 \omega} \qquad (16)$$

and

$$P(\omega) = -\frac{C_{11} + 2C_{12}(f_2/f_1)\omega + C_{22}(f_2/f_1)^2\omega^2}{2(1 + (f_2/f_1)^2\omega)^2} + \mathcal{O}(\rho_1) \qquad (17)$$

In the above derivation we have assumed that the polymer molecules are free in the solution, so that they scatter light individually. When the end-functionalized polymer is added into the colloidal suspension, some of the polymer molecules adsorb on the surface of the colloidal particle and form the polymer–colloid micelles. If all the polymer molecules adsorb on the colloidal surfaces (complete adsorption), the mixture can be viewed as a single-component polymer–colloid micelle system. In this case the standard virial expansion for the scattering light intensity is still valid. The only change required is to express the scattering amplitude of the polymer–colloid micelle in terms of its two constituents. Therefore, eq 13 becomes[5]

$$BM_1\rho'_1/R(0) = \frac{1}{(1 + (f_2/f_1)\omega)^2}\left\{ 1 - \frac{\rho'_1}{M_1} C_{33}(0) + \mathcal{O}(\rho_1^2) \right\} \qquad (18)$$

In the above, $-C_{33}(0)/2$ is the second virial coefficient for the polymer–colloid micelles, and the scattering amplitude of the polymer–colloid micelle is assumed to be $f_1 + \omega f_2$, with f_1 and f_2 being the scattering amplitudes for the colloidal particle and the polymer molecule, respectively. One can immediately see that the intercept $Y(\omega)$ in eq 18 decays much faster than that in eq 16 ($f_2/f_1 \simeq 0.1$ for our colloid–polymer mixture). This difference in $Y(\omega)$ reflects the fact that while the scattering from the polymer and colloid within the micelles is coherent, it is incoherent if the polymer molecules are not adsorbed onto the colloidal particles. The slope $P(\omega)$ is a measure of the "interaction volume" of the mixture. When there is no adsorption in the colloid–polymer mixture, the total interaction volume

of the mixture is an intensity-normalized sum of the individual excluded volumes (i.e., the second virial coefficients) of a colloidal particle and a polymer molecule as well as the excluded volume between the two species. For the complete adsorption, on the other hand, the interaction volume is just the excluded volume of the polymer–colloid micelle.

In the case where there is only a fraction of polymer molecules adsorbed on the colloidal surfaces, the colloid–polymer mixture can be viewed as a two-solute system consisting of the polymer–colloid micelles and free polymer molecules. Equation 13 can still be used to calculate the total scattering intensity of the mixture, except one has to use $f_3 = f_1 + \alpha \omega f_2$ as the scattering amplitude of the polymer–colloid micelle and $(1 - \alpha)\rho'_2$ as the free polymer concentration. Notice that α is independent of ω and is a function of ρ'_1 only ($\alpha = \gamma \rho'_1$; see eq 9). In the partial adsorption case, the intercept $Y(\rho'_2)$ in eq 13 has the form

$$Y(\rho'_2) = \left(\frac{f_3}{f_1}\right)^2 - \frac{(1-\alpha)\rho'_2}{M_2}\frac{2f_2}{f_1}C_{12} =$$
$$1 + \frac{\rho'_2}{M_2}\frac{2f_2}{f_1}(\gamma M_1 - C_{12}) + \mathcal{O}(\rho_2{}^2) \quad (19)$$

Equation 19 together with eq 14 can be used to measure the polymer partition coefficient α.

If the polymer-to-colloid molar ratio $\omega = \rho_2/\rho_1$, instead of ρ_2, is used as an independent variable, the intercept $Y(\omega)$ has the same functional form as that in eq 16, and the slope $P(\omega)$ becomes

$$P(\omega) = -\frac{\gamma M_1 \omega (2f_2/f_1 - (f_2/f_1)^2)}{2(1 + (f_2/f_1)^2\omega)^2} -$$
$$\frac{C_{33} + 2C_{32}(f_2/f_1)\omega + C_{22}(f_2/f_1)^2\omega^2}{2(1 + (f_2/f_1)^2\omega)^2} + \mathcal{O}(\rho_1) \quad (20)$$

where the free polymer is denoted as component 2 and the polymer–colloid micelle is denoted as component 3. The first term in eq 20 is the contribution from changes of the scattering amplitude of the polymer–colloid micelles. The second term, which has a similar functional form to eq 17, is due to the interactions in the mixture, as we discussed above. The interaction parameters C_{ij} in eq 20 are functions of $\rho_1\omega$ (i.e., ρ_2) and can be approximated as

$$C_{33} = C_{11} + \mathcal{O}(\rho_1\omega), \quad C_{32} = C_{12} + \mathcal{O}(\rho_1\omega) \quad (21)$$

Therefore, at low colloid concentrations the change of the scattering light intensity due to the interactions for the partial adsorption case is approximately the same as that for the nonadsorption case.

It should be pointed out that the above calculations assume that there are only two types of scattering species: free polymer chains and polymer micelles with colloidal cores. Such a division might seem natural since the polymer–colloid micelles all scatter much more light than the free polymer chains do. In our actual system, however, the free polymer chains are monodispersed in size, but the polymer–colloid micelles differ from each other in numbers of adsorbed polymer chains, which has been discussed in section 2.1. We now argue that the above formulas for a two-solute monodispersed system can still be used in our polydispersed system, as long as proper averaged quantities are used. When the concentration of the polymer–colloid micelles is moderately low, the size and the position of the micelles can be assumed to be uncorrelated.[15] The scattering intensity then becomes a product of the average form factor and the average structure factor. The poly-

dispersity in particle sizes mainly affects the structure factor through a modification of its wave vector (Q) dependence, which we can ignore since the measurements, to be discussed below, are performed at the small Q limit. In this case a cumulant expansion method[15] can be used to relate the average form factor to the mean size of the polydispersed scatterers. Here, the detailed shape of the distribution is not important and the scattering from the mixture of free polymer chains and the polydispersed polymer–colloid micelles can be viewed as coming from free polymer chains and a collection of mean-sized micelles. In this quasi-two-solute system, the polymer–colloid micelles have an average scattering amplitude of $f_1 + \langle \alpha\omega \rangle f_2$, where the average number of adsorbed polymer molecules per colloidal particle is

$$\langle \alpha\omega \rangle = \sum_{n=0}^{\infty} n x_n \Big/ \sum_{n=0}^{\infty} x_n \quad (22)$$

Notice that in the above argument we have used the fact that the intensity average $\langle (f_1 + \alpha\omega f_2)^2 \rangle$ is approximately equal to the amplitude average $f_1 + 2\langle \alpha\omega \rangle f_1 f_2$, when the scattering amplitude ratio f_2/f_1 is small. This condition is met in our light scattering experiment, to be described below.

3. Experiment

The colloidal particle chosen for the study consists of a calcium carbonate (CaCO$_3$) core with an adsorbed monolayer of a randomly branched calcium alkylbenzene sulfonate (CaSA) surfactant. The monolayer has a thickness[16] of 19 ± 1 Å. The synthesis procedures used to prepare the colloidal dispersion have been described by Markovic et al.[16] These colloidal particles have been well-characterized previously using small-angle neutron and light scattering techniques[5,16] and are used as an acid-neutralizing aid in lubricating oils. Such a nonaqueous dispersion is ideal for the investigation attempted here since the colloidal system is approximately a hard-sphere system.[17] Our dynamic light scattering measurements[5] revealed that the colloidal particles had a hydrodynamic radius of 5.0 nm and that the size polydispersity was approximately 10%. The molecular weight of the colloidal particle $M_1 = 300\,000 \pm 15\%$, which was obtained from a sedimentation measurement.[5] The colloidal samples for scattering studies were prepared by dispersing known amounts of the concentrated material in decane. The colloidal suspension then was centrifuged at 10^5 g (10^7 cm/s^2) for 2.5 h in order to remove any colloidal aggregates and dust.

The polymer used in the study was hydrogenated polyisoprene, i.e., alternating poly(ethylene–propylene) (PEP) and its single-end-functionalized derivatives, which were synthesized by the anionic polymerization scheme.[11,18,19] One derivative contains a tertiary amino group capped at one end of the chain (amine-PEP). The second has a strongly polar sulfonate–amine zwitterion at the end of the chain (zwitterion-PEP). The parent PEP and its end-functionalized derivatives are model polymers, which have been well-characterized previously using various experimental techniques.[11,18,19] Molecular weight characterization was carried out by size-exclusion chromatography, which was made with a Waters 150-C SEC instrument using μ-Styragel columns and tetrahydrofuran as the elution solvent. The ratio M_w/M_n was well below 1.1 for samples in the study. It was found that decane was a good solvent for both the colloid and the polymers. The zwitterion-PEP polymer was cleaned by dissolving it in hexane, filtering the polymer–hexane solution with a 0.45-μm duropore (Millipore brand) filter, and then evaporating the hexane. The unfunctionalized PEP and amine-PEP were used as received because they were clean.

Light scattering measurements were performed using a Brookhaven Instruments light scattering goniometer (BI-200SM). A 30-mW He/Ne laser (Spectra Physics, Model 127) illuminated a 10-mL sample cell in an index-matching vat. The laser intensity was stable within 2% over a day. Toluene was used as an index-matching fluid to reduce stray scattering from the glass wall of
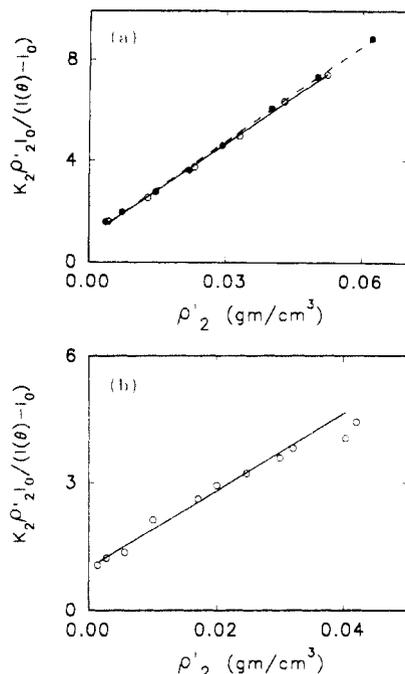
Figure 1. Plots of $K_2\rho'_2/(I(\theta)/I_0 - 1)$ versus ρ'_2 for PEP (closed circles in a), amine-PEP (open circles in a), and zwitterion-PEP (open circles in b) in decane. The solid and dashed lines are linear fits to the data points. The scattering angle θ = 90°.

Table I. Characterization of the Colloidal Particle and the Polymers in Decane (i = 1 for Colloid and i = 2 for Polymer)

sample	b_{ii}/M_i (cm^3/g)	R_{ii} (nm)	K_i ($\times 10^2$)	f_2/f_1
M_1 = 300 000	3.8	4.8	8.1	
$(M_2)_f$ = 26 000	62.8	5.4	1.32	0.12
$(M_2)_a$ = 25 000	61.2	5.3	1.54	0.13
$(M_2)_z$ = 25 000	512.0	10.8	17.45	1.43

the sample cell. All the measurements were conducted at room temperature. The scattered light coming from a well-defined scattering volume and angular aperture was collected by a photomultiplier (EMI 9863/350). Intensity measurements were accumulated automatically for 2-s periods at various scattering angles θ.

4. Results and Discussion

4.1. Characterization of Polymer and Colloid.
Figure 1a presents the scattering data for PEP with molecular weight $(M_2)_f$ = 26 000 (solid circles) and for amine-PEP with $(M_2)_a$ = 25 000 (open circles). (A subscript outside the parentheses is used to identify a quantity, which is related to different polymers. Letters f, a, and z are used for free, amine, and zwitterion throughout this paper.) The data are plotted as $K_2\rho'_2/(I(\theta)/I_0-1)$ versus ρ'_2, where $I(\theta)$ is the scattering intensity from the polymer solution at a concentration ρ'_2 (g/cm^3), measured at a scattering angle θ, and I_0 is the light intensity scattered from the solvent alone (ρ'_2 = 0). Since the size of the polymer molecules (see Table I) is much smaller than the wavelength of the incident light (λ = 623.8 nm), the measured $I(\theta)$ is independent of θ. It is seen from Figure 1a that the two sets of data are almost the same, indicating that there is no association for the amine-PEP polymer. This conclusion was also drawn by Davidson et al. in a study of the association behavior of the same end-functionalized polymers.[11] The value of b_{22}/M_2 (b_{22} and M_2 being the second virial coefficient and the molecular weight of the polymer molecules, respectively) is determined from the slope of the fitted straight line. The solid and dashed lines in Figure 1a are the linear fits to the data points.
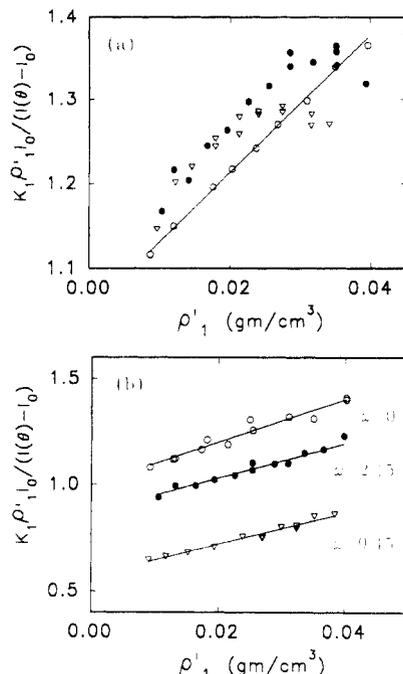
Figure 2. Plots of $K_1\rho'_1/(I(\theta)/I_0 - 1)$ versus ρ'_1 for the colloidal mixtures with different polymers in decane at θ = 90°. (a) The colloid-PEP mixture with ω = 3 (open circles), ω = 4.82 (closed circles), and ω = 15.3 (open triangles). The solid line is a linear fit to the data points with ω = 3. (b) The colloid-amine-PEP mixture with ω = 0 (open circles), ω = 2.15 (closed circles), and ω = 9.45 (triangles). The solid lines are the linear fits to the data points.

With the measured b_{22} one can define the radius R_{22} of an equivalent hard sphere via $4(4\pi/3)R_{22}^3 = b_{22}$. In general, $R_{ij} = 0.39(b_{ij})^{1/3}$, where the subscript ij denotes the species. Notice that the constant K_2 in the plot of Figure 1a was chosen such that $K_2\rho'_2/(I(\theta)/I_0 - 1) = 1$ when $\rho'_2 = 0$. Similarly, a constant K_1 for the colloidal particles is obtained and will be used to normalize other scattering data from the colloid-polymer mixture. The ratio $(b_{22}/M_2)_a/(b_{22}/M_2)_f$ of the two virial coefficients should be equal to $((M_2)_a/(M_2)_f)^{0.764}$ according to theory[20] and a recent experiment.[18] The measured $(b_{22}/M_2)_a/(b_{22}/M_2)_f$ = 0.97, which agrees well with the expected value ($(25/26)^{0.764}$ = 0.97). It is known from eq 13 that the ratio $K_1/K_2 = (f_1^2/M_1)/(f_2^2/M^2)$, where f_1 is the scattering amplitude of a colloidal particle, and f_2 is for a polymer molecule. With this equation the value of f_2/f_1 can be obtained. In Table I the measured values of f_2/f_1 for the different polymers are listed. Here we have used the fact that both f_1 and f_2 have the same sign (positive) relative to the solvent, which was checked using a Chromatix KMX-16 laser differential refractometer.[5]

The zwitterion-PEP chains are found to associate strongly in decane. Figure 1b shows the scattering data for the zwitterion-PEP with $(M_2)_z$ = 25 000. The solid line in Figure 1b is the fitted function $1 + 90.4\rho'_2$. The constant $(K_2)_z$ in the plot is found to be much larger than $(K_2)_a$. From the ratio of the two constants (see Table I), we find the average association number $n = (K_2)_z/(K_2)_a$ = 11.3. Similar association behaviors for the zwitterion-PEP were also found in other organic solvents.[11] Table I lists the measured values of b_{ii}/M_i and the corresponding hard-sphere radii for our polymers and the colloid in decane.

4.2. Scattering from Colloid-Polymer Mixtures.
We now discuss the mixtures of the colloid and the polymers. Figure 2 shows plots of $K_1\rho'_1/(I(\theta)/I_0-1)$ versus ρ'_1 for the colloidal mixtures with different polymers in decane. The constant K_1 in the plot was chosen such that

$K_1\rho'_1/(I(\theta)/I_0 - 1) = 1$ when $\omega = 0$. Figure 2a shows the effect of adding PEP at different molar ratios: $\omega = 3$ (open circles), $\omega = 4.82$ (closed circles), and $\omega = 15.3$ (open triangles). When the PEP is absent ($\omega = 0$), the data follow a straight line (see Figure 2b). From the slope of this line one obtains the second virial coefficient b_{11} for the colloidal particles. When PEP is added to the colloidal suspension, the colloidal particles experience an attraction due to the depletion effect, which is discussed in section 2. This attraction shrinks the linear region in the virial expansion. Therefore, the plot of $K_1\rho'_1/(I(\theta)/I_0 - 1)$ versus ρ'_1 becomes curved. This curvature effect is clearly shown in Figure 2a. It reveals that the linear region in the plot becomes smaller with an increasing ω, which indicates that the polymer-induced attraction between the colloidal particles is increased. The initial slope of the plot is also increased with ω, a characteristic that is predicted by eq 17.

The curvature effect does not appear when the amine-PEP is added to the colloidal solution. This indicates a suppression of the depletion-induced attraction between the colloidal spheres. In fact, the colloidal suspension is stabilized by the adsorption of the amine-PEP polymer onto the colloidal surfaces, as we will discuss below. Figure 2b shows the scattering data measured in the colloid–amine-PEP mixture at three molar ratios: $\omega = 0$ (open circles), $\omega = 2.15$ (closed circles), and $\omega = 9.45$ (triangles). The solid lines are the fitted functions: $1 + 10.0\rho'_1$ (top), $0.87 + 8.2\rho'_1$ (middle), and $0.57 + 7.4\rho'_1$ (bottom). The scattering data measured in the colloid–zwitterion-PEP mixture are similar to those shown in Figure 2b. One striking feature of Figure 2 is that the scattering intensity at the smallest colloidal concentration $\rho'_0 = 0.01$ g/cm^3 varies considerably when the amine-PEP is added to the colloidal suspension (Figure 2b) but hardly at all for the colloidal mixture with PEP (Figure 2a).

In Figure 2 the measured $BM_1\rho'_1/R(0)$ is plotted as a function of ρ'_1, when ρ'_1 is in the range between 0.01 and 0.04 g/cm^3. At a finite colloid concentration $\rho'_1 = \rho'_0$, one can introduce an "intercept"

$$F(\omega,\rho'_0) \equiv BM_1\rho'_0/R(0) = Y(\omega) + (2\rho'_0/M_1)P(\omega) \qquad (23)$$

from which the polymer partition coefficient α at ρ'_0 can be obtained. Figure 3 shows the measured $F(\omega,\rho'_0)$ as a function of ω at the fixed $\rho'_0 = 0.01$ g/cm^3 for the colloidal mixtures with PEP (open circles in a), amine-PEP (closed circles in a), and zwitterion-PEP (open circles in b). For the unfunctionalized PEP the measured $F(\omega,\rho'_0)$ is almost a constant, whereas for the two end-functionalized polymers $F(\omega,\rho'_0)$ decreases with increasing ω. The large decrease in $F(\omega,\rho'_0)$ indicates an adsorption of the polymer molecules onto the colloidal surfaces. This is because the colloid–polymer complex scatters much more light than the colloid and polymer in their unassociated state, as we discussed in section 2.

The upper solid curve in Figure 3a is a fit to eq 23 with $f_2/f_1 = 0.12$. Equations 16 and 17 are used to calculate $Y(\omega)$ and $P(\omega)$, respectively. The interaction parameters C_{11}, C_{12}, and C_{22} in eq 17 are treated as fitting parameters in the plot. The equation for the colloidal mixture with the nonadsorbing polymer fits the data well. Our previous study of the same system has also shown that the PEP polymer does not adsorb onto the colloidal spheres.[5] For the two end-functionalized polymers, it is found that they are partially adsorbed onto the colloidal surfaces. The lower solid curve in Figure 3a is a fit to eq 23, with $Y(\omega)$ and $P(\omega)$ being calculated using eqs 16 and 20, respectively. The values of the interaction parameters C_{11}, C_{12}, and C_{22}
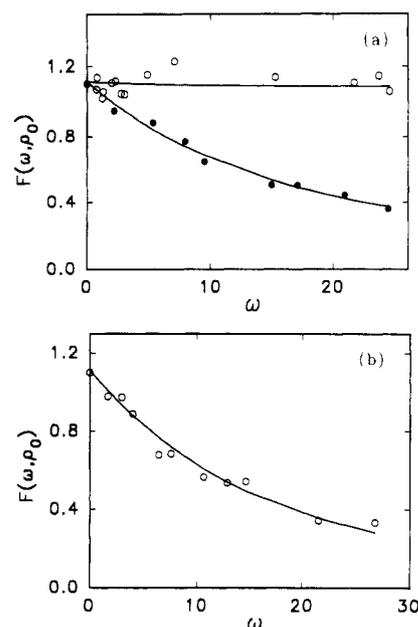
Figure 3. Measured $F(\omega,\rho'_0)$ as a function of ω for the colloidal mixtures with PEP (open circles in a), amine-PEP (closed circles in a), and zwitterion-PEP (open circles in b). The solid curves are the least-squares fits to the data points (see text).

used in the fitting are those for the mixture of the colloid and free polymer obtained from the upper solid curve. Thus there is only one fitting parameter in the plot, namely, the coefficient γ. From the fitting we find $\gamma = 23 \pm 3$ cm^3/g, and hence $\alpha = \gamma\rho'_0 = 0.23 \pm 0.03$ when $\rho'_0 = 0.01$ g/cm^3. In the concentration range $\rho'_1 \leq 0.02$ g/cm^3, the fitted value of γ is found to be a constant independent of the molar ratio ω and the colloid concentration ρ'_1, which agrees with the theoretical calculation shown in eq 9. At higher colloid concentrations, however, one needs to introduce a higher order term proportional to $\rho'_1\omega$ in eq 20 in order to fit the data in the whole range of ω and to obtain a consistent value of γ. Such a higher order correction can be attributed to changes of the interaction parameters in the mixtures of the colloid and the functionalized polymers, as is shown in eq 21.

Similarly, we find that the zwitterion-PEP data can also be fitted to eq 23, with $Y(\omega)$ and $P(\omega)$ being given in eqs 16 and 20, respectively. The solid curve in Figure 3b shows the fitting with a constant $\gamma = 25 \pm 3$ cm^3/g. Thus, the polymer partition coefficient $\alpha = \gamma\rho'_0 = 0.25 \pm 0.03$ when $\rho'_0 = 0.01$ g/cm^3. The interaction parameters used in the fitting are the same as those for the amine-PEP data. It is known from Figure 1b that the zwitterion-PEP molecules form polymer micelles in the pure polymer solution. We do not know at this stage whether the polymer micelles retain their identities upon mixing with the colloidal particles. However, the data fitting suggests that the zwitterion-PEP molecules in the colloidal mixture behave like the amine-PEP molecules and that the polymer partition coefficients for the two polymers have almost the same value.

The measurements shown in Figures 2 and 3 were performed using the colloid concentration ρ'_1 and the polymer-to-colloid molar ratio ω as the two independent variables. We also carried out measurements in the colloid–amine-PEP mixture using the colloid and polymer concentrations, ρ'_1 and ρ'_2, as experimental control parameters. Figure 4 shows the measured $Y(\rho'_2)$ as a function of ρ'_2 for the colloid–PEP mixture (solid circles) and the colloid–amine-PEP mixture (open circles). It is seen that the measured $Y(\rho'_2)$ for the amine-PEP is larger than that for the PEP. The solid curve in Figure 4 is a least-squares
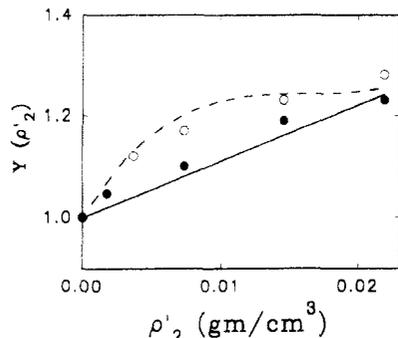
Figure 4. Variations of the intercept $Y(\rho'_2)$ as a function of the polymer concentration ρ'_2 for the colloidal mixtures with PEP (closed circles) and with amine-PEP (open circles). The solid and the dashed curves are the least-squares fits to the data points (see text).

fit to eq 14 with an initial slope of 10 cm³/g. The dashed curve shows the fit to eq 19 with an initial slope of 45 cm³/g. By comparing the fittings with eqs 14 and 19, we find $\gamma = 11 \pm 9$ cm³/g. The substantial error in γ is largely due to the uncertainties in determining the intercept $Y(\rho'_2)$. Unlike the case presented in Figure 3, the intercept here changes by, at most, 20%. This is because the relative change of the scattering intensity in the colloid–polymer mixture becomes very small, when the colloid concentration approaches zero. Since the intercepts, themselves, can only be determined with 10% accuracy, we expect Figure 4 to have limited value in determining the exact value of γ. Still, the measurements in Figure 3 and 4 show a qualitative agreement. One can use $\gamma = 11 \pm 9$ cm³/g to find $\alpha = 0.11 \pm 0.09$ when $\rho'_0 = 0.01$ g/cm³. We note only that this value of α is of the same order of magnitude as that obtained from Figure 3a.

4.3. Estimation of the Adsorption Isotherm and Energy. With the fitted values of α, one can obtain the adsorption isotherm, which is a plot of the number of the adsorbed polymer molecules per colloidal particle ($\alpha\omega$) versus the polymer–colloid molar ratio ω. Because α is a constant independent of ω in our working range of ω, the adsorption isotherm is then a simple linear function of ω, with the slope being α. The maximum value of $\alpha\omega$ obtained for our end-functionalized polymers is 6, which is smaller than the geometrical packing limit for the polymer molecules whose size is comparable to that of the colloidal particles (the coordination number is 8 for a simple body-centered-cubic lattice). In this weak adsorption limit, the polymer–colloid interaction can be described by an equilibrium constant. The polymer molecules partition themselves between the bulk fluid and the adsorbed state. The partition coefficient α is proportional to the amount of colloid and depends exponentially on the free energy of adsorption, as is shown in eq 9. The configuration of the adsorbed polymer on the colloidal surface is expected to be approximately a random coil with one end stuck on the surface. In the opposite limit where the amount of the polymer is much larger than that of the colloid, we expect the adsorbed amount of polymer per colloidal particle to reach some saturating value. At some point further attachment of polymer chains to the colloid is inhibited by a lack of attachment sites or by repulsion from the already attached polymer molecules.

The adsorption energy, ϵ, can be calculated using eq 10 when the polymer partition coefficient α is known. It is found that $\epsilon \simeq 4.5 k_B T$ for the amine-PEP when $\alpha = 0.23$. If $\alpha = 0.11$ is taken (see Figure 4), the corresponding $\epsilon \simeq 3.6 k_B T$. In the calculation of ϵ, we have taken $R_{11} = 4.8$ nm, $\delta = 2R_{22} = 10.6$ nm, $\phi_1 = 8.3 \times 10^{-3}$, and $N \simeq 25000/70$

$= 357$, where the monomer weight of the amine-PEP is 70. It should be pointed out that the change of the conformational entropy, ΔS, in eq 5 for a polymer chain adsorbed on a sphere of similar size is calculated using the scaling result for the polymer adsorption on a flat surface. This approximation is supported by a recent computer simulation,[21] which shows that a single polymer chain with one end stuck on the colloidal surface is approximately a random coil even when the size of the polymer coil becomes comparable to that of the colloidal particle. For the zwitterion-PEP the obtained free energy difference $\epsilon - f_0 \simeq 4.6 k_B T$, which is approximately the same as that for the amine-PEP.

In the previous study[5] of interactions in the mixture of the colloid and the unfunctionalized PEP, we found that the interaction between the colloid and the PEP is repulsive. The present study considers the effect of polar end groups on the polymer chains. In hydrocarbon solvents such end groups are expected to reduce the solubility of the polymers. In fact, we find that the zwitterion-PEP forms polymeric micelles in decane. In addition, the polar groups are found to interact attractively with the polar cores of the colloidal particles. The attractive potential energy ϵ is approximately $4 k_B T$. The obtained adsorption energy, $\epsilon - f_0$, between the zwitterion group and the colloidal surface is small compared with that when the colloidal surface is replaced by a bare mica surface.[22] In the latter case the adsorption energy different $\epsilon - f_0$ was estimated[23] to be $9 k_B T$. Presumably, the colloid–polymer attraction is mitigated by the surfactant corona around the colloidal particles. The amount and nature of the net attraction in hydrocarbon solvents, however, is an important open question.

4.4. Colloidal Interactions in Unfunctionalized and End-Functionalized Polymer Solutions. As we discussed in the Introduction, colloidal suspensions can be stabilized by the adsorption of the end-functionalized polymers on the colloidal surfaces. In particular, the adsorbed polymer can suppress the depletion attraction between the colloidal particles, since the polymer depletion zone surrounding a colloidal particle is modified by the adsorbed polymer. The stabilization of our colloidal mixture with the end-functionalized polymers is observed in a simple phase study. Three colloidal mixtures were prepared with different polymers: PEP, amine-PEP and zwitterion-PEP. The three samples have the same colloid concentration (9% by weight) and the same polymer concentration (5.3% by weight). The three polymers have approximately the same molecular weight ($M_w \simeq 25\,000$). It was observed that the sample with PEP phase separated, as is expected for the depletion effect. The other two samples were clear, and no sign of phase separation was observed.

Our light scattering scheme not only is capable of measuring the amount of the polymer adsorbed on the colloidal surface but also can probe changes of the microscopic interaction between the colloidal particles due to the polymer adsorption. Figure 5 shows the measured $P(\rho'_2)/M_1$ as a function of ρ'_2 for the colloid–PEP mixture (closed circles) and the colloid–amine-PEP mixture (open circles). The lower solid line in Figure 5 is the fitted function $3.4(1 - 51\rho'_2)$. The intercept of the linear function is just the second virial coefficient $b_{11}(0)/M_1$ for the colloidal particles measured at $\rho'_2 = 0$ (see the discussion about eq 15). The obtained value (=3.4 cm³/g) from the fitting agrees with our previous measurements.[5] The slope $P(\rho'_2)$ for a binary hard-sphere system can be calculated using eq 15. The expansion coefficients in eq 15 have
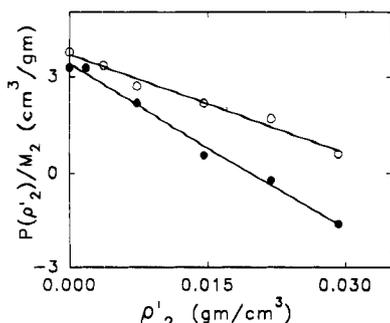
Figure 5. Measured slope $P(\rho'_2)/M_1$ as a function of the polymer concentration ρ'_2 for the colloidal mixtures with PEP (closed circles) and with amine-PEP (open circles). The solid lines are the linear fits to the data points.

been calculated in ref 5. For the mixture with R_{22} = 5.5 nm, R_{11} = 4.8 nm, and M_2 = 26 000, the calculated $P(\rho'_2)/b_{11}(0) = (1 - 46\rho'_2)$, which agrees well with the measurement.[5] The data in Figure 5 thus demonstrate that the binary hard-sphere model[3,24] can indeed describe the depletion effect in our colloid–PEP mixture.[5]

One can also view the colloid–amine-PEP mixture as a two-solute system consisting of the polymer–colloid micelles and the free polymer chains. Equation 15 is still valid when the solutes are composite objects. The only change required is to replace f_1 by $f_1 + \alpha\omega f_2$ and ρ'_2 by $(1 - \alpha)\rho'_2$. The upper solid line in Figure 5 is the fitted function 3.7 $(1 - 27.4\rho'_2)$. The effective slope of the linear function is $27.4/(1 - \alpha) = 36$, which is a factor of 0.7 smaller than that for the colloid–PEP mixture. A smaller slope for $P(\rho'_2)/b_{11}(0)$ indicates that the polymer adsorption reduces the depletion attraction between the colloidal particles. However, there is still some attraction between the colloidal particles due to the unadsorbed polymer molecules in the solution. This is shown by the decreasing trend of $P(\rho'_2)$ with an increasing polymer concentration.

5. Conclusion

A static light scattering method is developed to study the adsorption of single-end-functionalized polymers on colloidal spheres. With a model which combines features of the polymer adsorption and thermodynamics of the micellar aggregation, we calculate the adsorption energy ϵ between the end-functional group and the colloidal surface as a function of the polymer partition coefficient α, which is the probability for a single polymer chain to anchor to the colloidal surface. Using a virial expansion method for binary mixtures, we also calculate the concentration dependence of the small-angle light scattering intensity in colloidal mixtures with adsorbing polymer chains. With the obtained formulas one can measure the polymer partition coefficient α and then compute the adsorption energy ϵ. The scattering scheme also shows how the light scattering data provides information about changes of the microscopic interactions in the colloid–polymer mixtures.

In the experiment the monodispersed hydrogenated polyisoprene (PEP) and its single-end-functionalized derivatives were used to modify the interaction between the polymer and the colloidal surface. The experiment reveals that only a fraction of the end-functionalized polymers is adsorbed on the colloidal surface. The results for the end-functionalized polymers are compared with those for the unfunctionalized polymer. Since the interaction between the colloid and the unfunctionalized polymer is repulsive,[5] the adsorption of the end-functionalized polymers on the colloid has to occur through the functional end groups interacting attractively with

the polar cores of the colloidal particles. The adsorption energy between the functional group and the colloidal surface is estimated to be $\sim 4k_BT$. The experiment shows that the presence of the adsorbed polymer on the colloidal surfaces greatly reduces the depletion attraction between the colloidal particles and, therefore, enhances the stability of the colloid–polymer mixture. However, there is still some residual attraction between the colloidal particles due to the unadsorbing polymer molecules in the solution. Such an attractive interaction should be taken into account in studies of polymer-induced stabilization of the colloid. The experiment is of interest to observe the microscopic interaction between the colloid and polymer and to see how it responds to the incorporation of a functional group on the polymers. With this knowledge, one can estimate the phase stability properties in a straightforward way. To characterize subtle adsorption and interactions in colloid–polymer mixtures like those studied here is an experimental challenge. The present study shows that, in favorable cases, our scattering method is useful for measuring the adsorption of polymer molecules in colloidal suspensions.

References and Notes

(1) Cohen-Stuart, M. A.; Cosgrove, T.; Vincent, B. *Adv. Colloid Interface Sci.* **1986**, *24*, 143.
(2) Napper, D. H. *Polymeric Stabilization of Colloidal Dispersions*, Academic Press: New York, 1983.
(3) Vrij, A. *Pure Appl. Chem.* **1976**, *48*, 471.
(4) Asakura, S.; Oosawa, F. *J. Chem. Phys.* **1954**, *22*, 1255.
(5) Tong, P.; Witten, T. A.; Huang, J. S.; Fetters, L. J. *J. Phys. (Paris)* **1990**, *51*, 2813.
(6) Van der Beer, G. P.; Cohen-Stuart, M. A. *J. Phys. (Paris)* **1988**, *49*, 1449.
(7) Borkovec, M.; Eicke, H.-F.; Ricka, J. *J. Colloid Interface Sci.* **1989**, *131*, 366.
(8) Rao, I. V.; Ruckenstein, E. *J. Colloid Interface Sci.* **1987**, *119*, 211.
(9) de Gennes, P.-G. *Scaling Concepts in Polymer Physics*; Cornell University Press: Ithaca, NY, 1979.
(10) Eisenriegler, E.; Kremer, K.; Binder, K. *J. Chem. Phys.* **1982**, *77*, 6296.
(11) Davidson, N. S.; Fetters, L. J.; Funk, W. G.; Graessley, W. W.; Hadjichristidis, N. *Macromolecules* **1988**, *21*, 112.
(12) Bug, A. L. R.; Cates, M. E.; Safran, S. A.; Witten, T. A. *J. Chem. Phys.* **1987**, *87*, 1824.
(13) Wang, Z.-G. *Langmuir* **1990**, *6*, 928.
(14) Berne, B. J.; Pecora, R. *Dynamic Light Scattering*; Wiley: New York, 1976.
(15) Kotlarchyk, M.; Chen, S.-H. *J. Chem. Phys.* **1983**, *79*, 2461.
(16) Markovic, I.; Ottewill, R. H.; Cebula, D. J.; Field, I.; Marsh, J. F. *Colloid Polym. Sci.* **1984**, *262*, 648. Markovic, I.; Ottewill, R. H. *Colloid Polym. Sci.* **1986**, *264*, 65.
(17) Markovic, I.; Ottewill, R. H. *Colloid Polym. Sci.* **1986**, *264*, 454; *Colloids Surf.* **1987**, *24*, 69.
(18) Davidson, N. S.; Fetters, L. J.; Funk, W. G.; Hadjichristidis, N.; Graessley, W. W. *Macromolecules* **1987**, *20*, 2614.
(19) Mays, J.; Hadjichristidis, N.; Fetters, L. J. *Macromolecules* **1984**, *17*, 2723. Fetters, L. J.; Graessley, W. W.; Hadjichristidis, N.; Kiss, A. D.; Pearson, D. S.; Younghouse, L. B. *Macromolecules* **1988**, *21*, 1644. Mays, J.; Fetters, L. J. *Macromolecules* **1989**, *22*, 921.
(20) Le Guillou, J. C.; Zinn-Justin, J. *Phys. Rev. Lett.* **1977**, *39*, 95.
(21) Grest, G. S., private communication.
(22) Taunton, H. J.; Toprakcioglu, C.; Fetters, L. J.; Klein, J. *Nature* **1988**, *332*, 712.
(23) Ligoure, C.; Leibler, L. *J. Phys. (Paris)* **1990**, *51*, 1313.
(24) De Hek, H.; Vrij, A. *J. Colloid Interface Sci.* **1981**, *84*, 409.